

This is a repository copy of *Exotic decay of Cs 115*.

White Rose Research Online URL for this paper:

<https://eprints.whiterose.ac.uk/id/eprint/209127/>

Version: Published Version

---

**Article:**

Das, P., Datta, Ushasi, Chakraborty, S. et al. (30 more authors) (2023) Exotic decay of Cs 115. Physical Review C. 064304. ISSN: 2469-9993

<https://doi.org/10.1103/PhysRevC.108.064304>

---

**Reuse**

This article is distributed under the terms of the Creative Commons Attribution (CC BY) licence. This licence allows you to distribute, remix, tweak, and build upon the work, even commercially, as long as you credit the authors for the original work. More information and the full terms of the licence here:

<https://creativecommons.org/licenses/>

**Takedown**

If you consider content in White Rose Research Online to be in breach of UK law, please notify us by emailing [eprints@whiterose.ac.uk](mailto:eprints@whiterose.ac.uk) including the URL of the record and the reason for the withdrawal request.

## Exotic decay of $^{115}\text{Cs}$

P. Das,<sup>1,2</sup> Ushasi Datta<sup>1b</sup>,<sup>1,2,\*</sup> S. Chakraborty,<sup>1,3</sup> A. Rahaman,<sup>1,4</sup> O. Tengblad,<sup>5</sup> B. K. Agrawal,<sup>1,2</sup> A. Becerril,<sup>5</sup> J. Cederkall,<sup>7</sup> J. Dey,<sup>1,2</sup> A. Gottberg,<sup>6,8</sup> Sk Md Adil Imam,<sup>1,2</sup> M. Kowalska,<sup>6,9</sup> J. Kurcewicz,<sup>6</sup> M. Lund,<sup>10</sup> S. Mandal,<sup>11</sup> M. Madurga,<sup>6</sup> N. Marginean,<sup>12</sup> R. Marginean,<sup>12</sup> C. Mihai,<sup>12</sup> I. Marroquin,<sup>5</sup> E. Nacher,<sup>5</sup> A. Negret,<sup>12</sup> S. Pascu,<sup>12</sup> A. Perea,<sup>5</sup> E. Rapisarda,<sup>6</sup> F. Rotaru,<sup>12</sup> J. Ray,<sup>1</sup> P. Sharma,<sup>1</sup> T. Stora,<sup>6</sup> C. Sotty,<sup>12</sup> V. Vedia,<sup>13</sup> N. Warr,<sup>14</sup> and R. Wadsworth<sup>15</sup>

<sup>1</sup>Saha Institute of Nuclear Physics, Bidhannagar, Kolkata, India

<sup>2</sup>Homi Bhabha National Institute, Anishanktinagar, Mumbai, India

<sup>3</sup>University of Engg. and Management, Kolkata, India

<sup>4</sup>Jalpaiguri Govt. Engg. College, Jalpaiguri, West Bengal, India

<sup>5</sup>Inst. de Estructura de la Materia, CSIC, Madrid, Spain

<sup>6</sup>ISOLDE, CERN, Geneva, Switzerland

<sup>7</sup>Lund University, Lund, Sweden

<sup>8</sup>TRIUMF, Vancouver, Canada

<sup>9</sup>University of Geneva, Geneva, Switzerland

<sup>10</sup>Aarhus University, Aarhus, Denmark

<sup>11</sup>University of Delhi, Delhi, India

<sup>12</sup>Horia Hulubei National Institute for Physics and Nuclear Engineering, Bucharest-Magurele, Romania

<sup>13</sup>Facultad de CC. Físicas, Universidad Complutense, CEI Moncloa, Madrid, Spain

<sup>14</sup>Institut für Kernphysik, Universität zu Köln, Köln, Germany

<sup>15</sup>University of York, York, North Yorkshire, United Kingdom



(Received 31 July 2022; revised 6 July 2023; accepted 11 October 2023; published 5 December 2023)

The detailed study of the  $\beta^+$ /EC decay of the very neutron-deficient and alpha-unbound nucleus  $^{115}\text{Cs}$  is presented. The measurement was performed at the ISOLDE, CERN where delayed charged particles and  $\gamma$  rays were detected. The observed delayed  $\gamma$  rays are in agreement with the previously reported characteristics  $\gamma$  rays of  $^{115}\text{Xe}$ . Based on the experimental observations, the tentative ground-state spin of  $^{115}\text{Cs}$  is suggested to be  $7/2^+$  or  $9/2^+$ . Furthermore, the measured decay branching ratio of delayed protons exceeds the previously reported value. Additionally, new delayed  $\alpha$ -branching ratio and several reconstructed proton and  $\alpha$ -unbound excited states of  $^{115}\text{Xe}$  are being reported for the first time. The properties of proton-unbound states at excitation energies from 3.9–7.9 MeV have been obtained by fitting the delayed proton spectrum via the Bayesian method. The measured lifetimes of these proton-unbound states are in the order of zeptoseconds.

DOI: [10.1103/PhysRevC.108.064304](https://doi.org/10.1103/PhysRevC.108.064304)

### I. INTRODUCTION

The study of nuclei at the limits of stability has recently become the central focus of nuclear structure research [1–3]. Nuclei near the drip line exhibit fascinating properties, including the breakdown of traditional magic numbers [4–8], the emergence of new magic numbers, the presence of PIGMY resonances [9–12], exotic decay phenomena [13–15], and the manifestation of cluster structures [16–18]. Investigating the nuclear properties of doubly magic heavy nuclei near the proton drip line provides valuable insights into the interaction

between neutrons and protons at the boundaries of nuclear stability [19–22]. The enhanced proton-neutron pairing interactions in heavier  $N = Z$  nuclei result in larger reduced  $\alpha$ -decay widths [23], which indicate the manifestation of  $\alpha$ -cluster formation [24]. Therefore, studying the different decay modes of nuclei around  $^{100}\text{Sn}$  provides valuable information about nuclear properties at the nuclear boundary [25]. The nuclei near the proton drip line exhibit a significant difference in binding energies between proton and neutrons. This large difference in binding energies results in a high- $Q$  value for  $\beta$  decay, allowing the excited states of the daughter nucleus to be populated above the particle threshold. Therefore, studying the spectroscopic properties of those unbound states provides valuable information about the nucleon-nucleon (n-n) interaction and its coupling to the continuum. Additionally, the impact of the proton skin thickness on decay of neutron deficient nuclei warrants further investigation. The region of nuclei with mass  $A \approx (100\text{--}120)$ , near the proton drip line, is predicted to be an island of cluster emitters [16]. While

\*ushasi.dattapramanik@saha.ac.in

Published by the American Physical Society under the terms of the [Creative Commons Attribution 4.0 International](https://creativecommons.org/licenses/by/4.0/) license. Further distribution of this work must maintain attribution to the author(s) and the published article's title, journal citation, and DOI.

evidence of the heavy cluster emission (such as  $^{14}\text{C}$ ) from nuclei such as  $^{222,224}\text{Ra}$  were observed [26,27], the emission of ( $^{12}\text{C}$ ) from  $^{114}\text{Ba}$  remains inconclusive [28,29] and necessitates additional investigation in this mass region. Another intriguing aspect of this mass region is the  $rp$  process, which is responsible for synthesizing neutron-deficient nuclei close to the proton drip line [30,31]. The major uncertainties in understanding the process remain largely due to ( $p, \gamma$ ) reaction rates. Due to experimental limitation, the calculated reaction rates are mainly used. Therefore, the level structure above proton threshold of the nuclei around this region is crucial in constraining the reaction rates and strength. But limited experimental data [32–35] are currently available, and further experimental studies are required to deepen our understanding.  $^{115}\text{Cs}$  is a nucleus that is both proton and  $\alpha$  unbound [36]. Only the delayed proton branching ratio and lifetime of  $^{115}\text{Cs}$  was reported earlier [33]. This study represents the first comprehensive investigation of the decay modes of  $^{115}\text{Cs}$ . After electron capture and/or  $\beta^+$  decay the excited states of the daughter nucleus  $^{115}\text{Xe}$  were populated above the thresholds of one and two protons or  $\alpha$  cluster, etc. So the possible decay channels would be  $\beta\gamma$ ,  $\beta p$ ,  $\beta p\gamma$ ,  $\beta 2p$ ,  $\beta 2p\gamma$ , and  $\beta\alpha$ , etc. In a previous conference proceedings [34], a preliminary report on experimental setup, raw spectrum, detector calibration of the measurement was provided. The lifetime of the nucleus was obtained from the time distribution of delayed proton events [34], which was in agreement with previously reported value [33]. In this paper, with complete data analysis, the delayed proton,  $\alpha$ -branching ratios and several reconstructed proton- and  $\alpha$ -unbound excited states of  $^{115}\text{Xe}$  are reported for the first time.

## II. EXPERIMENTAL SETUP

The experiment was performed at the ISOLDE, CERN. A pulsed beam of 1.4 GeV protons from the proton synchrotron booster (PSB) were directed at a lanthanum carbide target maintained at 60 kV. The radioactive ion beam (RIB) was produced by fragmentation-spallation reactions. The RIB was plasma ionized and extracted via a cold transfer line into the beam line kept at ground potential. The extracted radioactive Cs beam was mass separated ( $A = 115$ ) in the general purpose separator (GPS), and directed to the experimental setup and implanted on a carbon target with a thickness of  $20\text{ }\mu\text{g}/\text{cm}^2$  for the subsequent  $\beta$ -decay study. The experimental setup consisted of five double-sided silicon strip detectors (DSSDs), stacked with four PAD detectors, behind each DSSD, functioning as  $\Delta E$ -E telescopes and the bottom DSSD had no PAD behind it. The DSSDs were of different thicknesses. The low-energy protons ( $<2.5\text{ MeV}$ ),  $\alpha$  ( $<9.6\text{ MeV}$ ), and heavier clusters (for  $^{12}\text{C}$ ,  $<51\text{ MeV}$ ) can be fully stopped in the thin DSSD4 and DSSD6 (thicknesses of 65 and 67  $\mu\text{m}$ ), while the higher-energy protons ( $<8.4\text{ MeV}$ ) were fully stopped in the thick DSSD2 (525  $\mu\text{m}$ ). The fifth thick horizontal DSSD5 (1000  $\mu\text{m}$ ) was used for detection of the  $\beta$  particles. The solid angle coverage of DSSD1, DSSD2, DSSD4, DSSD5, DSSD6 were 7.3%, 8.8%, 8.8%, 14.8%, 6.1% of  $4\pi$ , respectively. The chamber was surrounded by four high-purity germanium

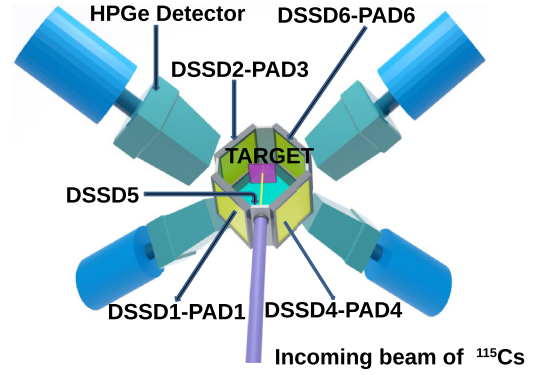


FIG. 1. The experimental (IS545) setup at ISOLDE.

(HPGe) clover detectors for detecting the  $\gamma$  rays. A schematic diagram of the experimental setup is shown in Fig. 1.

## III. DATA ANALYSIS

The data analysis was performed by using the CERNROOT platform. Calibration of the silicon detectors (thick and thin DSSD4, DSSD6, and PADs) and clover HpGe detectors was carried out using standard  $\alpha$  sources, ( $^{148}\text{Gd}$ ,  $^{241}\text{Am}$ ,  $^{239}\text{Pu}$ ,  $^{249}\text{Cf}$ ) and a  $\gamma$  source ( $^{152}\text{Eu}$ ) with known activity. The add-back algorithm was implemented to obtain the final  $\gamma$ -ray spectrum. Charged particles were identified using telescopes consisting of the DSSDs and PAD detectors. After the decay of  $^{115}\text{Cs}$ , the daughter nucleus  $^{115}\text{Xe}$  was populated with excitation energy up to 8.96 MeV, which was above the thresholds for emitting one proton, [ $S_p = +3.31(2)\text{ MeV}$ ], two protons [ $S_{2p} = +4.89(3)\text{ MeV}$ ], and  $\alpha$  [ $Q_\alpha = +2.51(1)\text{ MeV}$ ] [37]. This implies that the nuclei  $^{114}\text{I}$ ,  $^{113}\text{Te}$ , and  $^{111}\text{Te}$  could be populated by emitting a  $p$ ,  $2p$ , and an  $\alpha$ , respectively. Coincidence and anticoincidence measurements with consecutive PAD detectors were performed to separate delayed particles such as  $\beta$ ,  $\alpha$ ,  $p$ , etc. The coincidence spectrum between the thin DSSD and the consecutive PAD detector, shown in Fig. 2

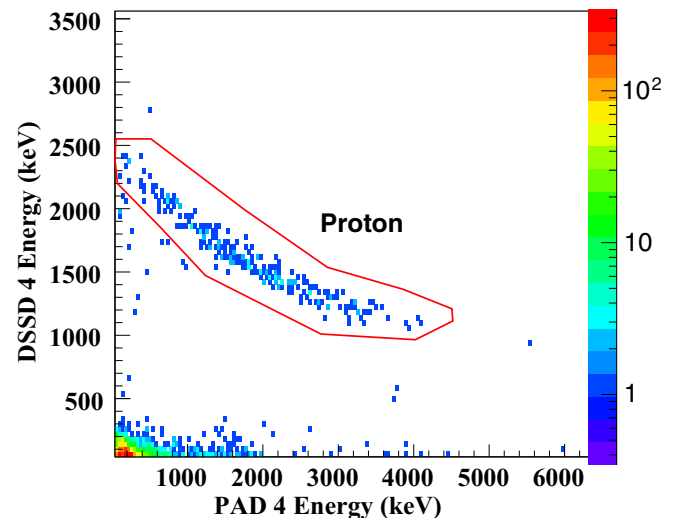


FIG. 2.  $\Delta E$ -E coincidence spectrum.

exhibits two distinct patches corresponding to protons and the  $\beta$ s. The unbound excited states of  $^{115}\text{Xe}$  were reconstructed by measuring the delayed protons and  $\alpha$ s. The delayed  $p$ -energy spectrum (from 2.5–5.66 MeV) was obtained by adding the deposited energies of the coincident events in the thin DSSD and the PAD detector. Conversely, the anticoincident events correspond to  $\alpha$  or heavy clusters, as well as protons with energies below 2.5 MeV. The bound states of  $^{115}\text{Xe}$  were also populated and identified by measuring of the energies of the deexcited  $\gamma$  rays, using clover detectors.

#### IV. RESULT AND DISCUSSION

The spin and parity of the ground state of  $^{115}\text{Cs}$  are unknown. For odd- $A$  Cs nucleus, it may depend upon the odd proton occupying orbital. But the situation is different depending on neutron occupation orbital. The ground-state spin of  $^{113}\text{Cs}$  is the  $3/2^+$ .  $^{117}\text{Cs}$  has two isomeric states with half-lives and spin parities as follows: 8.4(6) s;  $9/2^+$  and 6.5(4) s;  $3/2^+$ . Similarly,  $^{119,121,123}\text{Cs}$  also have an isomeric state close to the ground state. Based on the present experimental data analysis, it is observed that after the decay of  $^{115}\text{Cs}$ , the daughter nucleus was populated into three different types of excited states. Those states further decay by emitting  $\gamma$  rays, proton(s),  $\alpha$ (s), or heavy cluster(s).

##### A. Bound states of $^{115}\text{Xe}$

The ground-state spin and parity of  $^{115}\text{Xe}$  is tentatively known as the  $(5/2^+)$  [37]. The  $\beta$ -gated  $\gamma$ -ray spectrum shows several characteristics  $\gamma$  rays of  $^{115}\text{Xe}$ . The delayed  $\gamma$  transitions have energies 210(2) keV, 223(3) keV, 239(3) keV, and 349(5) keV. These transitions can be attributed to three strongly populated bands, originating from the  $\nu(g_{7/2}/d_{5/2})$ . The bands were extensively studied using in-beam  $\gamma$ -ray spectroscopy and fusion evaporation reaction [38]. The observed delayed  $\gamma$ -ray transitions from present experiment are consistent with previously reported transitions: 208(1) keV [ $7/2_1^+ \rightarrow (5/2_1^+)$ ], 220(1) keV [ $5/2^+ \rightarrow (5/2^+)$ ], 349(1) keV [ $9/2^+ \rightarrow (5/2^+)$ ] [38]. Additionally, a new  $\gamma$ -ray transition with an energy of 239(3) keV is observed, which may correspond to the decay from 241(2) keV ( $11/2^-$ ) to  $(5/2^+)$ . This possibility suggests the presence of octupole deformation in the nucleus. Figure 3 shows the  $\beta^+$ -gated  $\gamma$ -ray spectrum, where observed  $\gamma$ -ray transitions from  $^{115}\text{Xe}$  are labeled with the energies. The strong isomeric ( $T_{1/2} = 4.48$  h) decay transition [39],  $E_\gamma = 336$  keV from  $^{115}\text{In}$  has been observed in the background subtracted  $\gamma$ -ray spectrum. So, the main contaminant in the beam,  $^{115}\text{Cs}$  was accompanied by  $^{115}\text{In}$ . However, in the  $\beta$ -gated  $\gamma$ -ray spectrum, that  $\gamma$  line from  $^{115}\text{In}$  can be removed, and that nucleus has no delayed charge particle branch.

##### B. Unbound resonance states

The primary motivation of studying the decay mode of nuclei near the drip line is to investigate the population of the highly excited states, located above the particle threshold(s). To date, no particle-unbound states of  $^{115}\text{Xe}$  have been reported [36]. The unbound states of the daughter nucleus  $^{115}\text{Xe}$ ,

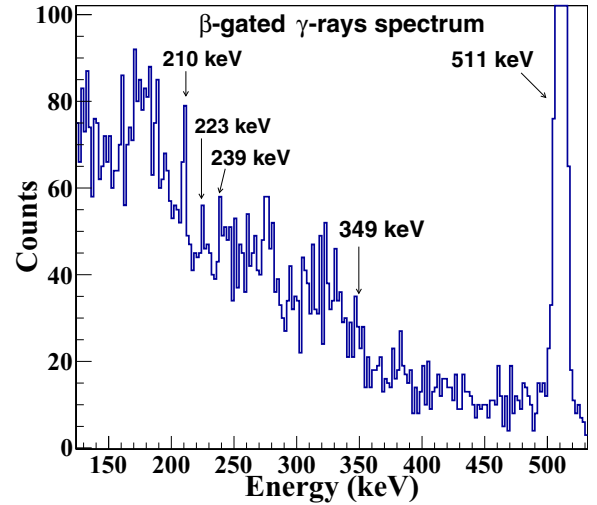


FIG. 3.  $\beta$ -gated  $\gamma$ -ray spectrum.

have been reconstructed. This reconstruction is achieved by analyzing the properties and characteristics of the emitted particles, such as delayed protons and  $\alpha$ s, as well as the  $\gamma$ -ray transitions observed in the decay process. More details are being described below.

##### 1. Proton-unbound states

The higher-energy part of the delayed proton spectrum has been obtained by adding the deposited energies of coincidence events in the thin DSSD and the PAD detectors. The low-energy protons ( $<2.5$  MeV) were fully stopped in the thin DSSD, which has been obtained from the thin DSSD spectrum in anticoincidence mode with the PAD detector. This low-energy spectrum has been added to the higher-energy part. The delayed proton spectrum has been converted into the reference frame of  $^{115}\text{Xe}$  and the proton separation energy has been added to extract the proton unbound excited states of  $^{115}\text{Xe}$ . Figure 4 (top) shows the proton-unbound excited states reconstructed from the present data without efficiency correction. The spectrum has been fitted with multiple Gaussian functions with variable widths via  $\chi^2$  minimization. This fit indicates the presence of six unbound states. The detector energy resolution has been considered to extract the widths of the states. Table I shows the energies and widths of the observed proton-unbound states. The relative population of unbound states are also mentioned in that table. The decay widths indicate the lifetime of these states and these are of the order of zeptoseconds. After the efficiency correction, the total number of delayed protons have been considered to obtain the delayed proton branch. According to our experimental data, the decay fraction of the delayed proton branch is 0.2(1)%, which is more than the previously reported value of 0.07% [33]. The  $\beta$  events were obtained from DSSD5 with efficiency correction. Total decay events were obtained by considering total  $\beta^+$  and EC/ $\beta$  ratio. The branching ratios of delayed particles have been obtained from the total decay events and corresponding delayed charged particles within t-proton gate



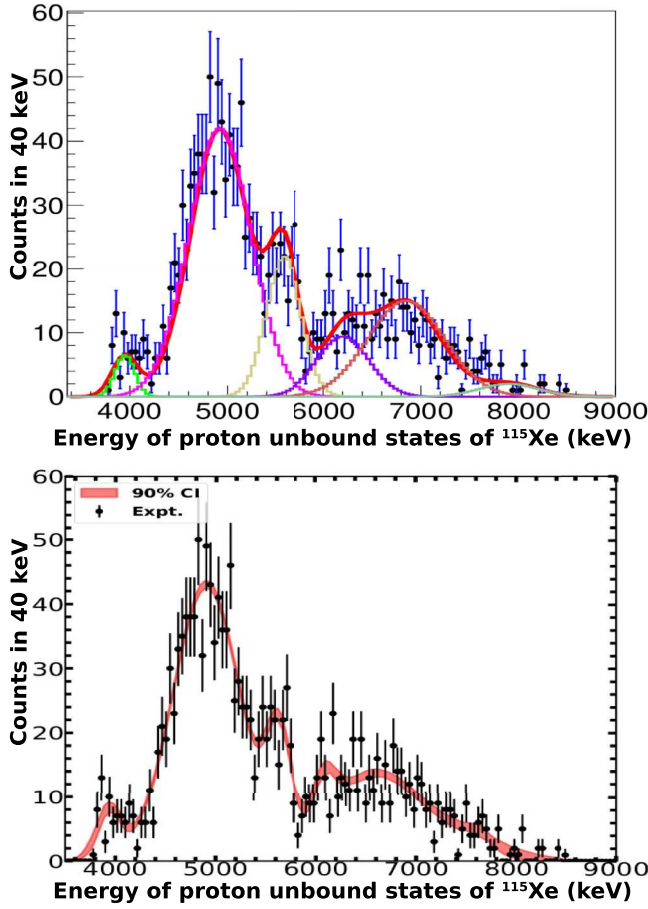


FIG. 4. (Top) The reconstructed proton unbound states of  $^{115}\text{Xe}$ . The solid line represents the fitted one by  $\chi^2$  minimization. (Bottom) The solid line represents the Bayesian method of analysis.

as 5 s. A better statistics is needed for delayed proton gated  $\gamma$  spectrum to explore further.

## 2. Bayesian estimation of parameters

The delayed proton spectrum has been fitted with Bayesian approach to obtain the properties of excited states [Fig. 4 (bottom)]. The approach is mainly based on the Bayes theorem,

TABLE I. Unbound states of  $^{115}\text{Xe}$ , fitted via  $\chi^2$  minimization and the Bayesian method (mentioned in the square brackets).

Energy of the unbound states (MeV)	Width keV	Measured lifetime zeptoseconds	Branching %	Delayed particle
3.9 [3.9]	289 [285]	2.3 [2.3]	0.006(1)	p
4.9 [4.9]	702 [787]	0.9 [0.8]	0.10(1)	p
4.9	422	1.6	0.005(1)	$\alpha$
5.6 [5.6]	364 [290]	1.8 [2.3]	0.030(2)	p
6.2 [6.1]	532 [262]	1.2 [2.5]	0.020(2)	p
6.8 [6.6]	817 [1079]	0.8 [0.6]	0.040(5)	p
7.9 [7.3]	690 [651]	1.0 [0.8]	0.005(1)	p
8.3	429	1.5	0.006(2)	$\alpha$

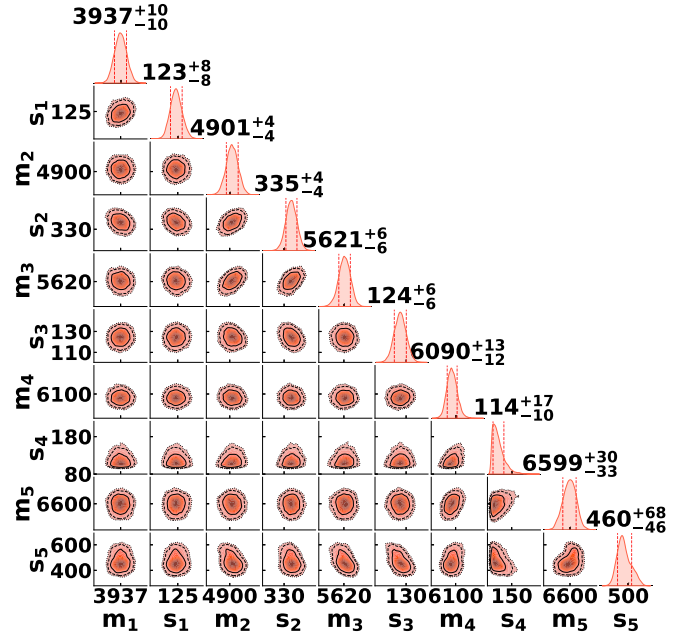


FIG. 5. Corner plot for correlation between partial parameters of the Bayesian analysis.

which states that [40],

$$P(\theta|D) = \frac{\mathcal{L}(D|\theta)P(\theta)}{\mathcal{Z}}, \quad (1)$$

where  $\theta$  and  $D$  denote the set of model parameters and the fit data, respectively. The  $P(\theta|D)$  is the joint posterior distribution of the parameters,  $\mathcal{L}(D|\theta)$  is the likelihood function,  $P(\theta)$  is the prior for the model parameters, and  $\mathcal{Z}$  is the evidence. To populate the  $P(\theta|D)$ , we implement a nested sampling algorithm by invoking the PYMULTINEST nested sampling [41] in the Bayesian inference library [42]. We use Gaussian likelihood function defined as,

$$\mathcal{L}(D|\theta) = \prod_j \frac{1}{\sqrt{2\pi}\sigma_j} e^{-\frac{1}{2}\left(\frac{D_j - M_j(\theta)}{\sigma_j}\right)^2}, \quad (2)$$

where the index  $j$  runs over all the data.  $D_j$  and  $\sigma_j$  are the data and corresponding uncertainties, respectively. The  $M_j$  are the model values that are obtained using the sum of the six Gaussian with their mean  $m_j$  and widths  $s_j$ , ( $i = 1, 2, \dots, 6$ ). The energies and widths (mentioned within square brackets) of those states from the Bayesian analysis are 3.90(1) [0.29] MeV, 4.9 [0.79] MeV, 5.6 [0.29] MeV, 6.10(1) [0.26] MeV, 6.60(3) [1.1] MeV, 7.3(3) [0.65] MeV. These values are very similar to those obtained by  $\chi^2$  fitting except the last few higher-energy states. The higher-energy proton unbound states have a broader energy distribution according to the Bayesian analysis. These values are given within the square brackets in Table I. Figure 5 shows the correlation of various fitted parameters, which are energies of the states ( $m_i$ ) and related widths ( $s_i$ ,  $i = 1, 2, 3, 4, 5, 6$ ). The diagonal plots in Fig. 5 show the univariate sample distribution of the parameters. Posterior mean and standard deviation are indicated in the figure. The off-diagonal plots show the kernel density

estimates (KDE) estimations of the bivariate posterior distributions of the parameters. From the corner plot, it is evident that the errors in the energies of the proton-unbound states are only few keV ( $\approx 0.1\%$ ) except for the higher-lying states ( $\approx 1\%$ ). On the other hand, the errors in the fitted widths of the unbound states are larger, ranging from 1–13 %. It is important to note that the fits that the energy of a particular state is correlated with the widths of the neighboring states, indicating overlapping widths of the states. Additionally, the lifetime of the states is of the order of zeptoseconds, which are shown within the square brackets in Table I. Although the results obtained from the standard method ( $\chi^2$  minimization) and the Bayesian analysis are somewhat similar but later method is free from any assumption on distribution of parameters, which is more acceptable. The information obtained on the proton-unbound states can provide valuable input for understanding open quantum many-body system calculations. The odd proton in the ground state of  $^{115}\text{Cs}$  may occupy either  $[404]9/2^+$  or  $[422]3/2^+$ . On the other hand, if the ground state of  $^{115}\text{Cs}$  is oblate [43], the tentative state, which can be occupied by the valence proton is  $[404]7/2^+$  or  $[413]5/2^+$ . The odd neutron of  $^{115}\text{Xe}$  may occupy  $[532]5/2^-$ , or  $[411]3/2^+$ , or  $[404]9/2^+$ . The ground-state spin and parity is known tentatively as  $(5/2^+)$  [33]. According to the present experimental observation, after decay it populates the bound state,  $7/2^+$  with a large branching ratio  $[31(6)\%]$ . So the probable ground-state spin of  $^{115}\text{Cs}$  can be  $7/2^+$  or  $9/2^+$ . A higher deformation ( $\beta_2 \approx 0.5\text{--}0.6$ ) is necessary to explain the higher-lying state(s) (7–8 MeV).

### 3. Cluster-unbound states

The study of the decay of  $^{115}\text{Cs}$  is fascinating due to the fact that the  $\alpha$  breakup threshold ( $Q_\alpha = +2.8$  MeV) [37] is lower than that of a single proton ( $S_p = -100$  keV). Similarly, the daughter nucleus  $^{115}\text{Xe}$  is also  $\alpha$  unbound, indicating the possible existence of an  $\alpha$ -cluster structure in the daughter nucleus. Therefore, conducting a detailed study of the quasi-bound  $\alpha$  states will be an important aspect of investigation. The ground state of the neighboring nuclei,  $^{113}\text{Xe}$  [44],  $^{114}\text{Cs}$  [45] have a known direct  $\alpha$ -decay probability. The  $\alpha$  separation energy of  $^{115}\text{Xe}$  is  $-2.506(14)$  MeV [35]. Hence, the expected energy range of delayed  $\alpha$  could be from 2.5–11.47 MeV.

By utilizing the anticoincidence of events between the thin DSSDs and the PADs, the energy spectrum above 2.61 MeV can be attributed to delayed  $\alpha$ . However, it is important to note that a portion of the observed  $\alpha$  strength could be originated from the direct  $\alpha$  decay of the ground state of  $^{115}\text{Xe}$ . To mitigate this contribution, appropriate analysis techniques have been employed. After implementing a t-proton gate of 5 s, some  $\alpha$  strength close to the ground state of  $^{115}\text{Xe}$  is still observed. This strength is concentrated around an energy of  $23_{-23}^{+42}$  keV. It is worth noting that the width of this  $\alpha$ -cluster state is comparable to the energy resolution of the DSSD. This suggests the presence of a narrow width quasi-bound state, which requires further investigation and analysis to fully understand its nature and properties. Let us clarify the information regarding the observed  $\alpha$ -cluster states of the daughter nucleus and the possibility of decay involving

TABLE II. Branching ratios of the delayed proton and  $\alpha$  of  $^{115}\text{Cs}$ .

Delayed Branch	Branching in %
proton	0.2(1)
$\alpha$	0.010(5)

heavier clusters. The energy spectrum above 6 MeV from the thick DSSDs (DSSD2 and DSSD5) (with t-proton gate as 5 s) can be considered as an  $\alpha$ -energy spectrum. In this spectrum, two peaks with statistically significant have been observed at 7.7(0.422) MeV and 11.3(0.429) MeV. These states can be attributed to  $\alpha$ -cluster states in the daughter nucleus. To obtain the excited cluster states, the measured spectrum was transformed into the center-of-mass (COM) frame, and the  $\alpha$  separation energy was subtracted. The resulting states were found to be at 4.9(0.4) MeV and 8.3(0.4) MeV, respectively. The widths of these states, considering the convolution of detector resolution, are mentioned in the brackets. Table I shows the energies with the widths of the observed  $\alpha$ -cluster states of the daughter nucleus. Table II provides the measured branching ratios of delayed proton and  $\alpha$  decay for  $^{115}\text{Cs}$ . Figure 6 shows a schematic diagram illustrating the detailed observed exotic decay of the  $^{115}\text{Cs}$ . An upper limit ( $<0.0034\%$ ) of  $^{12}\text{C}$  decay from  $^{114}\text{Ba}$  was measured [29]. Although the probability of such decay is very small, the positive  $Q$  values associated with the delayed clusters,  $^{12}\text{C}$ ,  $^{11}\text{C}$ , or  $^8\text{Be}$  (12 MeV, 4.7 MeV, and 4.9 MeV, respectively) suggests a further investigation for  $^{115}\text{Cs}$ . Due to experimental limitation, neither can be ruled out nor can be confirmed. The peak at 11.3 MeV could be due to delayed cluster ( $^{11}\text{C}$ , etc.) emission, then the probability would be 0.0002 (1)%. If the energy deposition at thick DSSD2 is considered due to  $^{11}\text{C}$ , then the energy of the unbound cluster state of  $^{115}\text{Xe}$  with configuration  $^{104}\text{Cd} \otimes ^{11}\text{C}$ , would be 5.6 MeV. A further dedicated investigation is necessary to confirm the emission of a heavy cluster.

## V. SUMMARY

The first detailed study of various decay modes of the proton- and  $\alpha$ -unbound nucleus,  $^{115}\text{Cs}$  is reported. The bound and unbound states of the daughter nucleus,  $^{115}\text{Xe}$ , were populated up to 8.3 MeV. Additionally, the measured branching ratios of delayed proton and  $\alpha$  decay for  $^{115}\text{Cs}$  are reported.

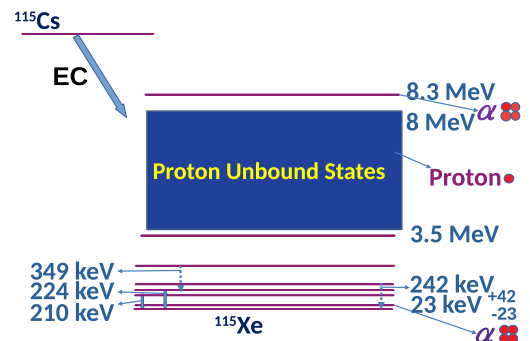


FIG. 6. Decay modes of  $^{115}\text{Cs}$ .

By employing the Bayesian method of analysis, several new proton-unbound states have been identified, characterized by very short lifetimes of the order of zeptoseconds. These findings have the potential to constrain calculations in the open quantum shell model for heavy nuclei, providing important insights into the behavior of exotic nuclear systems. Overall, this research sheds light on the decay mechanisms and nuclear structure, contributing to our understanding of rare and intriguing phenomena in nuclear physics.

### ACKNOWLEDGMENTS

The authors are thankful to the team members of the accelerator facility of CERN and RIB operation scientists at

ISOLDE, CERN for smooth operation of the experiment. We are sincerely thankful to Sukalyan Chattopadhyay for insightful comments and critical review of the manuscript. The present study was financially supported by SEND project grants (PIN:11-R&D-SIN-5.11-0400) from the Department of Atomic Energy (DAE), Govt. of India, the Project No. PID2019-104390GB-I00 by the Spanish Funding Agency (AEI/FEDER, EU), the German BMBF under Contract No. 05P21PKC11 and Verbundprojekt 05P2021 and ENSER2 (European Nuclear Science and Applications Research)-HORIZON 2020 Grant No 654002, Europe. P.D. acknowledges with thanks for the financial support provided by CSIR vide file number 09/489(0111)/2019-EMR-I.

- 
- [1] J. Erler *et al.*, *Nature (London)* **486**, 509 (2012).
  - [2] A. Miller *et al.*, *Nature Phys.* **15**, 432 (2019).
  - [3] G. A. Lalazissis, D. Vretenar, and P. Ring, *Nucl. Phys. A* **650**, 133 (1999).
  - [4] D. Suzuki *et al.*, *Phys. Rev. Lett.* **103**, 152503 (2009).
  - [5] L. Lalanne *et al.*, *Phys. Rev. Lett.* **129**, 122501 (2022).
  - [6] C. Thibault *et al.*, *Phys. Rev. C* **12**, 644 (1975).
  - [7] U. Datta *et al.*, *Phys. Rev. C* **94**, 034304 (2016).
  - [8] S. Chakraborty *et al.*, *Phys. Rev. C* **96**, 034301 (2017).
  - [9] N. Paar, D. Vretenar, and P. Ring, *Phys. Rev. Lett.* **94**, 182501 (2005).
  - [10] H. L. Ma, B. G. Dong, Y. L. Yan, H. Q. Zhang, and X. Z. Zhang, *Phys. Rev. C* **85**, 044307 (2012).
  - [11] A. A. Leistenschneider *et al.*, *Phys. Rev. Lett.* **86**, 5442 (2001).
  - [12] P. Adrich *et al.*, *Phys. Rev. Lett.* **95**, 132501 (2005).
  - [13] P. J. Woods and C. N. Davids, *Annu. Rev. Nucl. Part. Sci.* **47**, 541 (1997).
  - [14] M. J. G. Borge, *Phys. Scr.* **T152**, 014013 (2013).
  - [15] M. Pfützner, M. Karny, L. V. Grigorenko, and K. Riisager, *Rev. Mod. Phys.* **84**, 567 (2012).
  - [16] Yonghao Gao *et al.*, *Sci. Rep.* **10**, 9119 (2020).
  - [17] J. Ray *et al.*, *EPJ* **66**, 02089 (2014).
  - [18] U. Datta *et al.*, *AIP Conf. Proc.* **2038**, 020020 (2018).
  - [19] M. Mougeot *et al.*, *Nature Phys.* **17**, 1099 (2021).
  - [20] D. Lubos *et al.*, *Phys. Rev. Lett.* **122**, 222502 (2019).
  - [21] M. Górska, *Physics* **4**, 364 (2022).
  - [22] S. Frauendorf and A. O. Macchiavelli, *Prog. Part. Nucl. Phys.* **78**, 24 (2014).
  - [23] K. Auranen *et al.*, *Phys. Rev. Lett.* **121**, 182501 (2018).
  - [24] R. M. Clark *et al.*, *Phys. Rev. C* **101**, 034313 (2020).
  - [25] L. Capponi *et al.*, *Phys. Rev. C* **94**, 024314 (2016); R. D. Page, P. J. Woods, R. A. Cunningham, T. Davinson, N. J. Davis, A. N. James, K. Livingston, P. J. Sellin, and A. C. Shotton, *ibid.* **49**, 3312 (1994).
  - [26] H. J. Rose and G. A. Jones, *Nature (London)* **307**, 245 (1984).
  - [27] P. B. Price, J. D. Stevenson, S. W. Barwick, and H. L. Ravn, *Phys. Rev. Lett.* **54**, 297 (1985).
  - [28] C. Mazzocchi *et al.*, *Phys. Lett. B* **532**, 29 (2002).
  - [29] A. Guglielmetti *et al.*, *Phys. Rev. C* **56**, R2912(R) (1997); **52**, 740 (1995).
  - [30] V. V. Elomaa *et al.*, *Phys. Rev. Lett.* **102**, 252501 (2009).
  - [31] S. Lahiri and G. Gangopadhyay, *Int. J. Mod. Phys. E* **21**, 1250074 (2012).
  - [32] K. Auranen *et al.*, *Phys. Lett. B* **792**, 187 (2019).
  - [33] J. M. D'auria *et al.*, *Nucl. Phys. A* **301**, 397 (1978).
  - [34] P. Das *et al.*, *J. Phys.* **1643**, 012127 (2020).
  - [35] M. Wang and G. Audi, *Chin. Phys. C* **36**, 1603 (2012); **45**, 030003 (2021).
  - [36] <https://www.nndc.bnl.gov/>.
  - [37] J. Blachot, *Nucl. Data Sheets* **113**, 2391 (2012).
  - [38] E. S. Paul, H. R. Andrews, T. E. Drake, J. DeGraaf, V. P. Janzen, S. Pilotte, D. C. Radford, and D. Ward, *Phys. Rev. C* **53**, 2520 (1996).
  - [39] H. H. Hansen *et al.*, *Z. Phys.* **269**, 155 (1974).
  - [40] A. Gelman, J. B. Carlin, H. S. Stern, D. B. Dunson, A. Vehtari, D. B. Rubin, J. Carlin, H. Stern, D. Rubin, and D. Dunson, *Bayesian Data Analysis Third edition* (CRC Press, Boca Raton, 2013).
  - [41] J. Buchner, A. Georgakakis, K. Nandra, L. Hsu, C. Rangel, M. Brightman, A. Merloni, M. Salvato, J. Donley, and D. Kocevski, *Astron. Astrophys.* **564**, A125 (2014).
  - [42] G. Ashton *et al.*, *Astrophys. J. Suppl. Series* **241**, 27 (2019).
  - [43] M. Aggarwal, *Phys. Rev. C* **89**, 024325 (2014).
  - [44] S. Kumar *et al.*, *Nucl. Data Sheets* **137**, 1 (2016).
  - [45] G. Gürdal and F. G. Kondev, *Nucl. Data Sheets* **113**, 1315 (2012).